



UvA-DARE (Digital Academic Repository)

Understanding the complex dynamics of financial markets through microsimulation

Qiu, G.

Publication date
2011

[Link to publication](#)

Citation for published version (APA):

Qiu, G. (2011). *Understanding the complex dynamics of financial markets through microsimulation*.

General rights

It is not permitted to download or to forward/distribute the text or part of it without the consent of the author(s) and/or copyright holder(s), other than for strictly personal, individual use, unless the work is under an open content license (like Creative Commons).

Disclaimer/Complaints regulations

If you believe that digital publication of certain material infringes any of your rights or (privacy) interests, please let the Library know, stating your reasons. In case of a legitimate complaint, the Library will make the material inaccessible and/or remove it from the website. Please Ask the Library: <https://uba.uva.nl/en/contact>, or a letter to: Library of the University of Amsterdam, Secretariat, Singel 425, 1012 WP Amsterdam, The Netherlands. You will be contacted as soon as possible.

Chapter 5

Why Do Options Markets Smile?

As remarked in Chapter 3, many agent-based models for studying market dynamics have been developed in the last few decades, however, most of them focus on stock markets (see Chapter 4) and very few center on options markets. More importantly, one of the most challenging and puzzling problems in financial economics stems from options markets, namely the understanding of the origin of the volatility smile phenomenon. For a detailed discussion of this problem, we refer the reader to Chapter 2. Briefly, up till now, the reason for the volatility smile phenomenon remains unclear.

Moreover, across the globe, financial markets are currently in turmoil, in part due to speculative trading in derivatives. With current trading volumes exceeding \$530 trillion, derivatives have been labeled ‘financial weapons of mass destruction’ (Goodman (2008)). In an ideal market, derivative contracts are priced to eliminate risk (Black and Scholes (1973), Merton (1973)). In practice, however, many derivatives traders correct for market imperfections using ad-hoc, perturbative pricing schemes. The volatility smile is a key consequence of these imperfections in real markets. Ironically, this lack of understanding at a microscopic level turns the heuristics which had been developed to control risk, into new sources of unquantifiable risk, in particular at moments of abnormal market behavior, as evidenced by the current (2008-2009) financial crisis.

This fact has stimulated us to develop a microsimulation (MS) model of options markets capable of revealing the mechanisms underlying the volatility

smile¹.

Section 5.1 exhibits our MS model of options markets. In Section 5.2 the simulation results are presented. More detailed discussion on the mechanisms governing the shape and dynamic properties are presented in Section 5.3.

5.1 A microsimulation model of options markets

In options markets, there are three main types of trader: Hedgers, speculators, and arbitrageurs. Typically, hedgers use options as insurance to protect their financial interests, but do not attempt to gain profit from options markets; speculators trade options to bet on the future prices in the hope of making capital gains; and arbitrageurs involve making riskless profits by taking advantage of price disparities.

Traders are also different in their trading activity. Typically, hedgers only need to trade once in a certain period. In contrast, speculators are much more active due to the benefits of option trading, i.e., its power of leverage, namely gaining exposure to larger amounts of assets for a much smaller investment, and its potential to profit whether the underlying asset moves up or down. Arbitrageurs are even more active. There are many traders of this type in options markets and their trading will quickly eliminate any detected arbitrage opportunity. Consequently, price disparities are usually small and transient, arbitrageurs therefore need to trade frequently in order to lock-in significant profits.

The smile dynamics exhibits apparent regularity even on short (e.g., daily) time scales, as shown in Cont and da Fonseca (2002) and Fenger et al. (2003). We therefore consider that, whereas the smile is inevitably influenced by the less active traders, its basic dynamics should be accounted for by the behavior of the more active market participants. In fact, this is supported by some empirical studies: Natenberg (1994) stated that, in most options markets, arbitrageurs and speculators typically outnumber hedgers. Lakonishok et al. (2007) reported that little option volume can be attributed to hedging; instead, a significant fraction

¹This chapter is based on Qiu et al. (2010a) and Qiu et al. (2010b)

of option trading is speculative in nature and mainly motivated by views about the direction of future stock price movements. In modeling options markets, we hence focus on active traders, namely (directional) speculators and arbitrageurs.

In our model, the market participants trade in European call/put options on a single underlying asset with the identical time to maturity but with different strikes. There are N_{tr} traders and N_{op} call/put options. The strike price of the n -th call/put option is represented by K^n , and its market price at time t is denoted as $V^{n,\phi,t}$. Speculators make decisions based on their expectations of the asset price at the option expiration time. In addition, their expected prices are influenced by news over time. Arbitrageurs trade in response to different arbitrage opportunities. Inspired by the empirical fact that trading in out-of-the-money (OTM) options is more liquid than in-the-money (ITM) options (Ederington and Guan (2002)), a differential liquidity mechanism is introduced in the model. Change of option price is modeled as being proportional to excess demand, mimicking the action of market makers to balance supply and demand (see Appendix A.1). For the sake of simplicity, we ignore interest rate, dividends, transactions costs, taxes, and keep the time to maturity fixed. In the remaining part of this section, we describe the model in detail. In order to offer important insight into the smile phenomenon, we adopt an approach of successive complexification of the basic model, which is similar to that taken in Johnson et al. (2003) and Qiu et al. (2007).

5.1.1 S model: The market consists of only speculators

We start with the case that all the traders are speculators (SP). Our model at this stage is named ‘S model’. Each speculator has an idiosyncratic belief about the future price of the underlying asset. We denote the price of the underlying asset at the option expiration time as perceived by the i -th speculator at time t as $S_{SP}^{i,t}$. The current price of the underlying asset S^t , the fraction of speculators F_{SP}^t , and $S_{SP}^{i,t}$ are all influenced by news and vary over time. We denote the long-term mean of $S_{SP}^{i,t}$ as \bar{S}_{SP}^i and assume that, for the entire group of speculators, \bar{S}_{SP}^i follows a lognormal distribution (for the simple reason that prices cannot be negative). The mean of the distribution of $S_{SP}^{i,t}$ for the entire group of speculators

at time t is represented by M_{SP}^t and the corresponding standard deviation is denoted as D_{SP}^t . The difference between M_{SP}^t and S^t reflects the level of the speculators' anxiety about the price movement, while D_{SP}^t conveys the level of the speculators' disagreement about the future. For a more detailed description, see Appendix A.2.

At each time-step, based on their expected asset prices, the speculators estimate the profitability of trading each option. We assume that the transaction quantity of the i -th speculator for the n -th option, denoted as $Q_{SP}^{i,n,\phi,t}$, is proportional to the trader's expected profit of the deal:

$$Q_{SP}^{i,n,\phi,t} = \lambda_{SP} [\max(\phi(S_{SP}^{i,t} - K^n), 0) - V^{n,\phi,t}], \quad (5.1)$$

where λ_{SP} is a positive parameter indicating the activity level of the speculators and, at this stage of modeling, it is independent of strike. Here, $\max(\phi(S_{SP}^{i,t} - K^n), 0)$ is the payoff as estimated by the trader that can be gained from buying the option, while the price of the option $V^{n,\phi,t}$ represents the cost for establishing this long position. Therefore, if the former is greater/smaller than the latter, the trader will purchase/write the option.

5.1.2 SA model: The market consists of both speculators and arbitrageurs

Next, arbitrageurs (AR) are included. We name the model at this stage 'SA model'. The arbitrageurs monitor the option prices and trade those options found to violate the arbitrage relations, e.g., put-call parity (PCP) and butterfly spread (BFS) (Cox and Rubinstein (1985)). If these relations are violated, arbitrageurs will sell/buy the relatively overvalued/undervalued option(s). We assume that their transaction quantities are proportional to the strength with which the relations are violated.

PCP is an arbitrage relationship between the European call and put options with the identical strike price: $V^{n,1,t} - V^{n,-1,t} = S^t - K^n$ (Cox and Rubinstein, 1985). If it is violated, an arbitrageur's transaction quantity is

$$Q_{AR_{PCP}}^{i,n,\phi,t} = -\phi \lambda_{AR_{PCP}} (V^{n,1,t} - V^{n,-1,t} - S^t + K^n), \quad (5.2)$$

where $\lambda_{AR_{PCP}}$ indicates the activity level of the arbitrageurs for the PCP strategy and $V^{n,1,t} - V^{n,-1,t} - S^t + K^n$ expresses the strength of the PCP violation related to the n -th call and put options. By transacting the relatively under- and overvalued claims in equal amounts, a sure profit is expected to be guaranteed.

BFS stands for an arbitrage relationship involving three call/put options with strike prices that are separated by an equal distance: $V^{n,\phi,t} < (1/2)(V^{n-h,\phi,t} + V^{n+h,\phi,t})$ (Cox and Rubinstein (1985)). If this relation is violated, an arbitrageur's transaction quantity is

$$\begin{pmatrix} Q_{AR_{BFS}}^{i,n-h,\phi,t} \\ Q_{AR_{BFS}}^{i,n,\phi,t} \\ Q_{AR_{BFS}}^{i,n+h,\phi,t} \end{pmatrix} = \begin{pmatrix} 1 \\ -2 \\ 1 \end{pmatrix} \lambda_{AR_{BFS}} \max(V^{n,\phi,t} - \frac{1}{2}(V^{n-h,\phi,t} + V^{n+h,\phi,t}) + \varepsilon^h, 0), \quad (5.3)$$

in which $\lambda_{SP_{BFS}}$ is a parameter indicating the activity level of the arbitrageurs for the BFS strategy. Here a portfolio consisting of three options with strikes K^{n-h} , K^n , and K^{n+h} and relative weights 1:2:1 is expected to lead to a sure profit. The value of h varies, meaning that the arbitrageurs apply this rule to all the possible butterfly spreads of which K^n is the common middle strike. $\varepsilon^h \geq 0$ denotes the convexity of the curve considered by the arbitrageurs. For a typical convex IV curve, ε^h increases with increasing h . For simplicity, we adopt $\varepsilon^h = \alpha h$ where $\alpha \geq 0$. The term $\max(V^{n,\phi,t} - \frac{1}{2}(V^{n-h,\phi,t} + V^{n+h,\phi,t}) + \varepsilon^h, 0)$ expresses the strength of the BFS violation related to the three call/put options.

5.1.3 SAL model: Difference in liquidity is included

In real markets, the liquidity of options is not balanced across strikes (Ederington and Guan (2002)). In general, OTM options are more liquid than ITM options, implying that speculators trade in the former more actively than the latter. This difference in liquidity might stem from the trading behavior of speculators and the price characteristics of options. Generally, speculators prefer cheap and liquid options in order to achieve high leverage and fast conversion. The potential for higher leverage provided by OTM options, which are cheaper than their ITM

counterparts, attracts more speculators. Higher leverage thus leads to higher liquidity, which in turn pulls in even more speculative trading volume. This positive feedback effect ensures the relatively higher/lower liquidity of OTM/ITM options.

We therefore further include the difference in liquidity by introducing a strike dependence to the speculators' trading activity, which is an increasing/decreasing function of strike price for the call/put options:

$$\lambda_{SP}(K^n) = \eta_{SP}[\phi \tanh(\gamma(K^n - S^t)) + 1], \quad (5.4)$$

where η_{SP} and γ are positive parameters.

Notice that in constructing arbitrage portfolios, all the options involved must be traded simultaneously and in the specified proportions. Liquidity unbalancing is therefore not applicable to the arbitrageurs in our model. This complete version of the model is termed 'SAL model'.

5.2 Simulation results

In simulations a wide range of values are considered for the model parameters¹. Our main findings are robust in the sense that all the main characteristics of the resulting IV smile remain qualitatively unchanged. The parameter values corresponding to the results shown in this paper are discussed in Appendix A.3.

5.2.1 Shapes of the implied volatility curves

Here we present the option prices and the corresponding IV curves generated by our model at different levels, by keeping S^t , F_{SP}^t , and $S_{SP}^{t,t}$ (hence M_{SP}^t and D_{SP}^t) constant and equal to their respective long-term means.

¹In microsimulations, we often face the situation as described in Lux and Marchesi (2000): "In order to choose appropriate sets of parameter values, one would ideally like to calibrate the model by using relevant empirical observations on its various components. Unfortunately, we lack empirical estimates for all those parameters ..."

5.2.1.1 Implied volatility curves from the S model

Using the S model, if M_{SP}^t coincides with S^t , the option prices overlap with the corresponding BS prices and the resultant IV curve against strike is flat (data not shown). This can also be shown analytically (see Appendix B).

We then examine the IV smile in the case that $M_{SP}^t < S^t$. In this situation, the price of the underlying asset is considered by the speculators more likely to suddenly drop than to suddenly rise, in line with the nature of stock indices. (Notice that we have assumed a zero interest rate and ignored dividends.) As shown in Figures 5.1(a) and 5.1(b), the resultant prices of all call/put options are lower/higher than the corresponding BS prices. Consequently, the IVs of the call options are lower than the corresponding IVs for the put options. Obviously, the simulated option prices do not satisfy put-call parity.

5.2.1.2 Implied volatility curves from the SA model

As illustrated in Figure 5.1(c), the simulated option prices from the SA model satisfy both put-call parity and the butterfly spread relation. It can be observed that the speculators' trading and that of the arbitrageurs tend to move the option prices in opposite directions. Hence, the different strategies followed by the speculators and the arbitrageurs lead to a competing effect on the simulated option prices.

5.2.1.3 Implied volatility curves from the SAL model

In the simulations based on the SAL model, if the arbitrageurs only act on violation of put-call parity, we have obtained results as shown in Figures 5.1(e) and 5.1(f). Here we see that most of the simulated option prices satisfy put-call parity. In addition, the IVs of the options with strikes lower than S^t are higher than those IVs corresponding to the options with strikes higher than S^t . Here we can observe that the competition becomes unbalanced due to the difference in speculators' activity between OTM options and ITM options. However, the options do not satisfy the butterfly spread relation. Consequently, the IV curves are not convex as shown in empirical data.

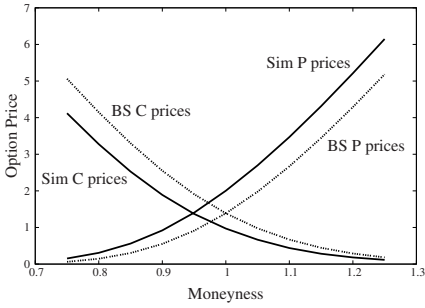
If the arbitrageurs also trade in response to violations of the butterfly spread relation, new competition is induced at some call and put options between the speculation and the butterfly spread arbitrage and also between the two types of arbitrage. At this point, as displayed in Figure 5.1(h), we have an IV skew similar to those observed in real markets for equity index options.

5.2.2 Dynamical properties of the implied volatility curves

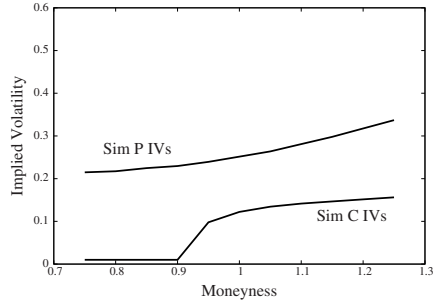
Based on the complete (SAL) model, we now consider the case that S^t , $S_{SP}^{i,t}$, and F_{SP}^t are all influenced by news and change over time. Figure 5.2(a) depicts the evolution of the IVs of three put options with different strike prices. Notice that the IVs are generally more volatile for small than large moneyness (K^n/S^t), in line with the empirical analysis reported in Cont and da Fonseca (2002). The transaction volumes for the call and put options are shown in Figure 5.2(b). Although we have adopted a simple activity function for the speculators, i.e. Equation (5.4), the resultant volume distribution is similar to the corresponding empirical distribution reported in Ederington and Guan (2002).

We then perform principal component analysis (PCA) on the resulting IV time series. Figure 5.2(c) exhibits the eigenvectors corresponding to the three largest eigenvalues. These principal components are in line with the empirical results reported in Cont and da Fonseca (2002) and Fengler et al. (2003). Figure 5.2(d) displays the proportions of variance explained by these eigenvectors. They agree with the empirical data from skew-dominated markets on the total variance explained by the first three eigenmodes and approximately on their relative values.

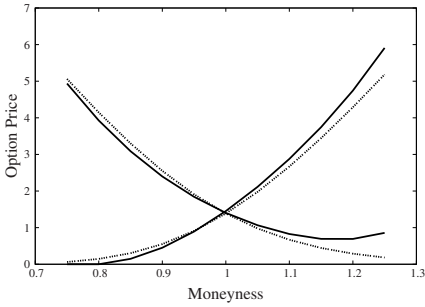
We have performed a sensitivity analysis of our model by varying the values chosen for some parameters that are critical to the simulated IV dynamics (see Section 5.4). It suggests that our results are qualitatively robust.



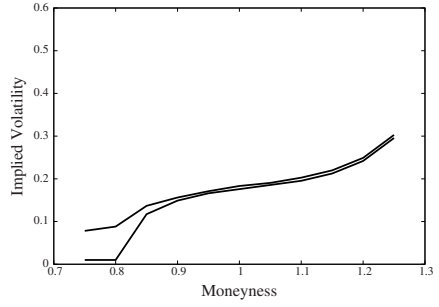
(a)



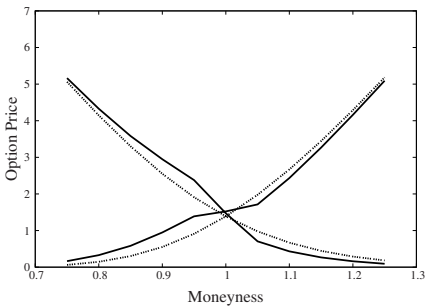
(b)



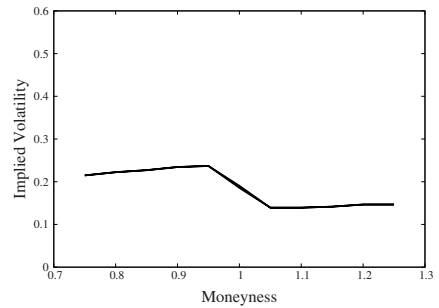
(c)



(d)



(e)



(f)

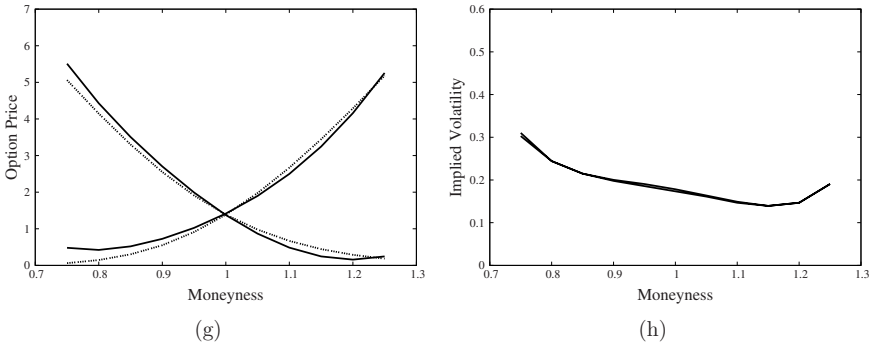


Figure 5.1: Simulated option prices and implied volatilities. They are plotted against moneyness (K^n/S^t) as solid lines (Sim is for ‘simulated’, C for ‘call’, and P for ‘put’). The corresponding BS prices (dashed lines), which satisfy all the arbitrage relations, are also plotted here for comparison. (a) Option prices obtained from the S model; (b) corresponding IVs. (c) Option prices obtained from the SA model; (d) corresponding IVs. (e) Option prices obtained from the SAL model if the arbitrageurs only act on violation of put-call parity; (f) corresponding IVs. (g) Option prices obtained from the SAL model if the arbitrageurs also act on violations of the butterfly spread relation; (f) corresponding IVs. A lower bound of 0.01 is taken for the IVs.

5.3 Discussion: The mechanism underlying the smile phenomenon

5.3.1 Competing effect induced by heterogeneous trading behavior

Figure 5.3 clarifies the competing types of trading behavior and their effects on the shape of the IV curves. It illustrates that, although the traders have distinct trading interests, their behavior leads to contests regarding the option prices and eventually the shape of the IV smile.

In the following parts of this section, we again keep S^t , $S_{SP}^{i,t}$, $F_{SP}^{i,t}$ constant

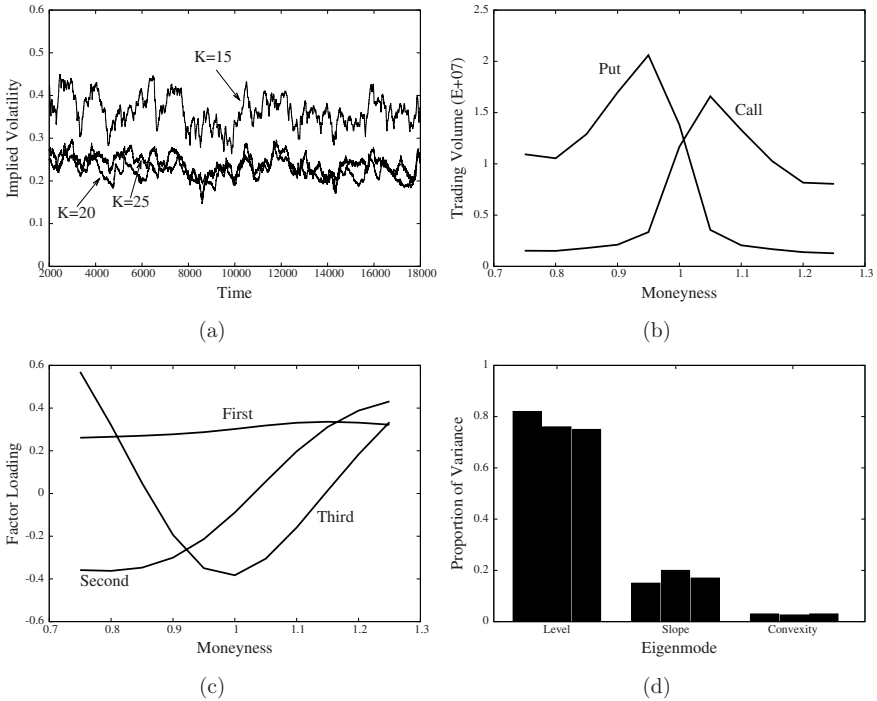


Figure 5.2: Dynamic results. (a) IV time series of the put options with different strike prices: $K = 15, 20,$ and 25 . (b) Trading volumes of the call and put options over the selected time period. (c) The eigenvectors corresponding to the three largest eigenvalues. (d) The proportions of variance explained by the principal components (first bar of each eigenmode): 82%, 15%, and 3%, respectively, in comparison with the empirical results shown in Fengler et al. (2003) (second bar) and our empirical findings.

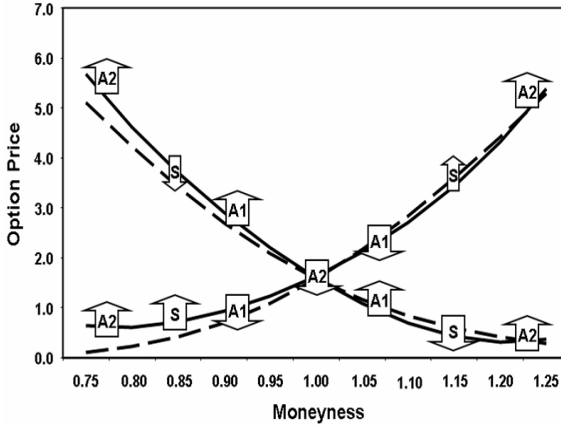


Figure 5.3: Competition. This figure exhibits the competition between the different types of trading behavior regarding the option prices. The S, A1, and A2 arrows represent, respectively, the effects of speculation, put-call parity arbitrage, and butterfly spread arbitrage. The larger/smaller S arrow denotes high/low speculators' activity level.

in order to investigate the influence of the variations in some individual free parameters of the model on the characteristics of the smile curve.

5.3.2 Shapes of implied volatility curves corresponding to different types of uncertainty

In financial markets, speculators have realized that large sudden positive and negative price changes are not equally likely to happen. Correspondingly, they will shift their expectations of the future price, to a certain extent, to the direction with higher possibility. Therefore the mean of the overall distribution of the expected prices will be generally away from the current price to that direction.

As shown in Figure 5.4, when $M_{S^t}^t < S^t$, we obtain a downward sloping IV curve; conversely, if $M_{S^t}^t > S^t$, we have an upward sloping one; if $M_{S^t}^t$ is close to S^t , the resultant curve is symmetric and turns upwards at both ends. The case

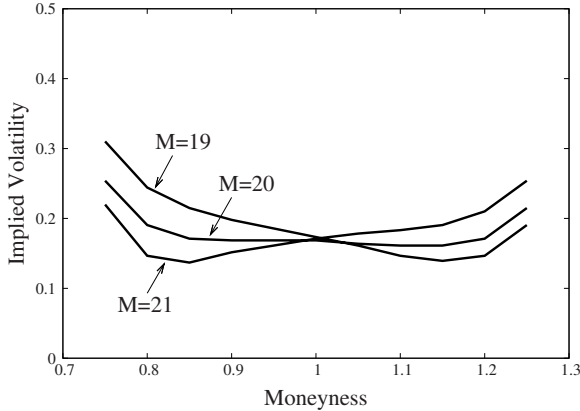


Figure 5.4: Shapes of IV curves. This figure presents the simulated IV curves corresponding to different values chosen for M_{SP}^t : 19, 20, and 21 respectively, while S_i is fixed at 20.

$M_{SP}^t < S^t$ indicates that the speculators believe that unexpected large price drops are more likely to happen than sudden large price rising. It reminds us of the nature of stock indices. This characteristic might only be realized by traders after a few large stock market crashes, e.g., the one happened in 1987. This explains why the smile has existed only since that crash. The situation $M_{SP}^t > S^t$ is similar to certain circumstances of some commodities, in which traders think that the prices might suddenly rise due to, eventually, the general shortage of resources. The case $M_{SP}^t \approx S^t$ resembles the situation of options on foreign exchange rates between currencies with equal strength, in which traders believe that the relative values of these currencies will change in a more symmetric way. The deviation of M_{SP}^t from S^t is therefore crucial to the shape of the IV curve.

5.3.3 Driving factors in the fluctuations of implied volatility curves.

As expressed in Figure 5.5(a), the smaller is M_{SP}^t with respect to S^t , the steeper is the skew. This may confirm the empirical observation that, whenever the market

declines/increases, the skew tends to become more/less pronounced (Hull (2003)). Our explanation is that, the more S^t falls, the further M_{SP}^t deviates from S^t due to ‘crashophobia’ (Rubinstein (1994)) and therefore the steeper the IV curve becomes. As shown in Figure 5.5(b), adopting larger/smaller values for D_{SP}^t , the IV curves are similar in shape but with higher/lower levels. This may confirm the empirical observation that scheduled news announcements generally lead to a drop of IVs; conversely, most major unscheduled announcements cause a rise (Ederington and Lee (1996)). Our explanation is that a scheduled/unscheduled announcement decreases/increases the variance of speculators’ expected prices, hence causes IVs to fall/rise. Figure 5.5(c) exhibits the effect of the competition between the speculators and the arbitrageurs: Speculation/(butterfly spread arbitrage) tends to decrease/increase the convexity.

We can further consider the heterogeneity of speculators with regard to the fear of large sudden price changes. In the case of equity index options, speculators are different in the degree of ‘crashophobia’ and in general pessimistic traders are more sensitive to negative news than optimistic traders. Then, the more the price of the underlying falls due to negative news, the larger D_{SP}^t becomes and consequently the more the IV curve rises. This can explain the so-called ‘leverage effect’ described in, e.g., Cont and da Fonseca (2002), that shifts in global level of IVs are negatively correlated with returns of the underlying. Contrary to index options, some speculators trading in commodity options are more sensitive than other traders to the news that triggers price rises. In this case, the more the price rise, the larger D_{SP}^t becomes and consequently the more the IV curve rises. This can confirm the ‘inverse leverage effect’ observed in commodity options markets, i.e., shifts in IV level are positively correlated with returns of the underlying (Geman (2005)).

When D_{SP}^t , M_{SP}^t , and F_{SP}^t vary together over time, the first two factors cause the most variation of the IV curve, as shown in Figure 5.2(d). We therefore conclude that the overall simulated dynamics is mainly driven by fluctuations in the level of speculators’ disagreement, as well as the level of their general anxiety about the price movement of the underlying asset.

In the next section, we will discuss some additional analysis that we have performed to demonstrate the robustness of our model.

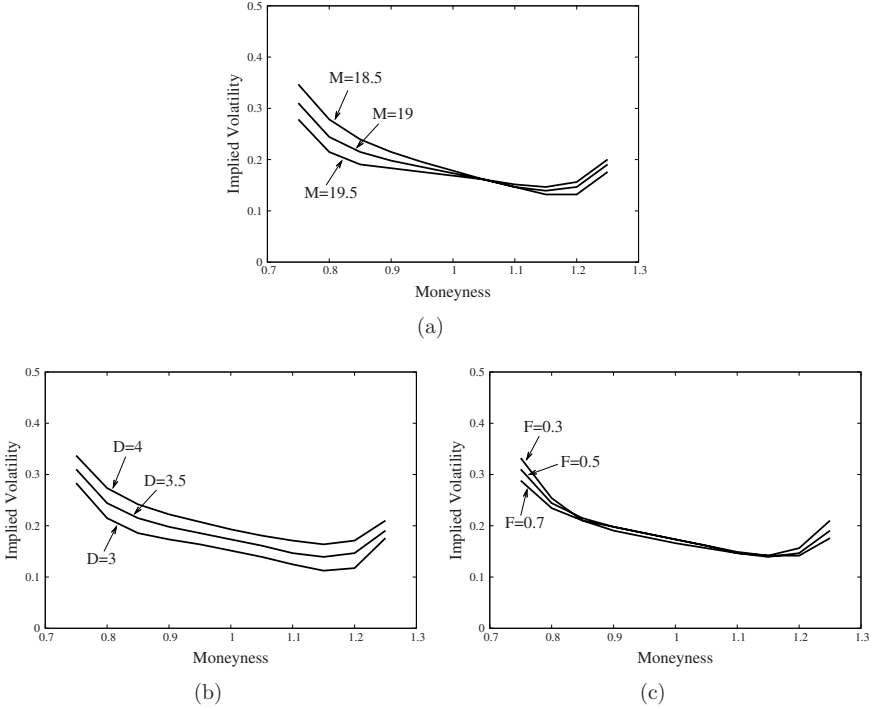


Figure 5.5: Driving factors of the IV dynamics. This figure shows the simulated IV curves corresponding to different values for M_{SP}^t , D_{SP}^t , and F_{SP}^t . Here, $S^t = 20$ and, unless otherwise indicated, the values for M_{SP}^t , D_{SP}^t , and F_{SP}^t are fixed at 19, 3.5, and 0.5 respectively. (a) $M_{SP}^t = 18.5, 19, \text{ and } 19.5$ respectively. (b) $D_{SP}^t = 3, 3.5, \text{ and } 4$ respectively. (c) $F_{SP}^t = 0.3, 0.5, \text{ and } 0.7$ respectively.

5.4 Robustness study

We have studied the robustness of our model by (1) investigating the variation in the shape of the IV smile due to speculative traders who use the Black-Scholes formula in assessing the option prices, and (2) examining the sensitivity of the IV dynamics to the variations in the model parameters.

5.4.1 Reactions of the implied volatility curve to speculations using the Black-Scholes model

In options markets, there are some speculators who employ (analytical) option pricing models, typically the BS formula. In valuing options, BS traders need to estimate the volatility of the underlying asset, which is the only unobservable parameter in the formula. For analyzing the robustness of our results, here we include some BS speculators in our model. For simplicity, we assume that these traders adopt strike-independent volatilities.

In real markets, BS speculators have different perceptions of the future volatility of the underlying asset. We express the volatility expected by the i -th speculator (if this trader is a BS speculator) as $\Sigma_{SP_BS}^{i,t}$ with a long-term average value $\bar{\Sigma}_{SP_BS}^i$. We assume that, for the entire group of BS speculators, $\bar{\Sigma}_{SP_BS}^i$ follow a lognormal distribution (for the simple reason that volatility cannot be negative).

At each time-step, based on their perceived volatilities, the BS speculators estimate the profitability of trading each option. We assume that the transaction quantity of the i -th speculator (who is a BS trader) for the n -th option is proportional to the trader's expected profit of the deal:

$$Q_{SP_BS}^{i,n,\phi,t+1} = \lambda_{SP_BS}(K^n) [V_{BS}^{\phi,t}(S^t, K^n, r, T, \Sigma_{SP_BS}^{i,t}) - V^{n,\phi,t}], \quad (5.5)$$

where $\lambda_{SP_BS}(K^n)$ is a positive parameter indicating the activity level of the BS speculators and, for simplicity, we assume $\lambda_{SP_BS}(K^n) = \lambda_{SP}(K^n)$;

$V_{BS}^{\phi,t}(S^t, K^n, r, T, \Sigma_{SP_BS}^{i,t})$ is the price of the option as expected by the BS trader; $V_{BS}^{\phi,t}(S^t, K^n, r, T, \Sigma_{SP_BS}^{i,t}) - V^{n,\phi,t}$ is therefore the payoff that can be gained from buying the option, while the price of the option $V^{n,\phi,t}$ represents the cost for establishing this long position. If the former is greater/smaller than the latter, the trader will purchase/write the option.

As shown in Figure 5.6(a), the BS speculators' trading can decrease the skewness of the IV curve produced by the directional speculators (through interactions with arbitrageurs). As the relative number of the BS traders is increased the steepness of the skew is further reduced. The flattening effect is expected because the BS speculators adopt strike-independent volatilities. Moreover, as shown in Figure 5.6(b), the higher the average perceived volatility of the BS traders, the higher the IV curve, vice versa.

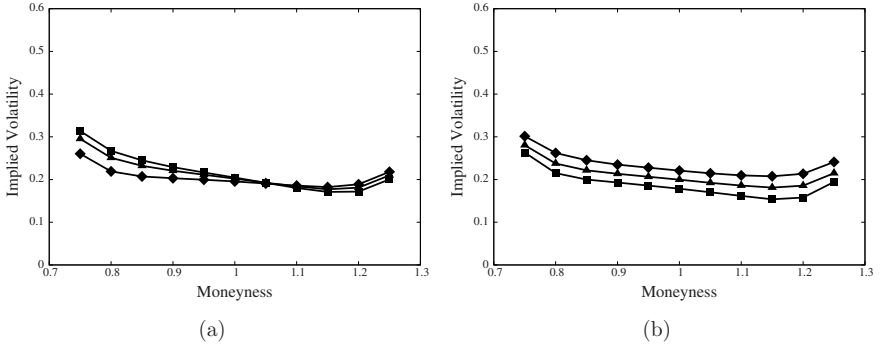


Figure 5.6: IV curves if the speculators using the BS model trade together with the simple directional (SD) speculators. The fraction of arbitrageurs is 30%. (a) The fractions of the BS speculators are 0% (the ■ line), 20% (▲ line), and 50% (the ◆ line) respectively. Here, the mean of the BS speculators' volatilities is 0.2. (b) The mean of the BS speculators' volatilities are 0.15 (the ■ line), 0.2 (the ▲ line), and 0.25 (the ◆ line) respectively. Here, the fraction of the BS speculators and that of the SD speculators are both 35%.

However, although the BS speculators can vary the skewness and level of the IV curve, the general shape of the curve remains unchanged. Further taking into consideration the fact that in reality directional speculators outnumber other types of speculator (Lakonishok et al. (2007)), the mechanism underlying the volatility smile revealed by our model is robust.

5.4.2 Sensitivity analysis of the implied volatility dynamics

Next, we vary the values chosen for some parameters that are critical to the simulated IV dynamics, i.e., ν_ψ , ν_ω , and ν_F , and examine the sensitivity of the IV dynamics to the variations in these parameters.

Table 5.1: Proportions of variance explained by the principal components corresponding to different values chosen for ν_ψ . All other parameters are kept fixed with $\nu_\omega = 0.02$ and $\nu_F = 0.05$.

ν_ψ	0.001	0.0015	0.002	0.0025	0.003
Level	0.87	0.85	0.82	0.80	0.77
Slope	0.09	0.12	0.15	0.17	0.20
Convexity	0.03	0.03	0.03	0.03	0.03

Table 5.2: Proportions of variance explained by the principal components corresponding to different values chosen for ν_ω . All other parameters are kept fixed with $\nu_\psi = 0.002$ and $\nu_F = 0.05$.

ν_ω	0.01	0.015	0.02	0.025	0.03
Level	0.56	0.72	0.82	0.88	0.92
Slope	0.36	0.22	0.15	0.10	0.07
Convexity	0.08	0.05	0.03	0.02	0.02

The results in Tables 5.1, 5.2, and 5.3 demonstrate that ν_ψ , ν_ω , and ν_F are positively correlated with the variance proportions explained by slope, level, and convexity respectively. This is in line with the mechanism discussed in Section 5.3.

Empirical studies have shown that the smile dynamics is characterized by three eigenmodes, among which level explains most of the variation of the smile, followed by slope and convexity (Cont and da Fonseca (2002), Fengler et al. (2003)). Our model robustly confirms this finding for a wide range of parameter settings.

Table 5.3: Proportions of variance explained by the principal components corresponding to different values chosen for ν_F . All other parameters are kept fixed with $\nu_\psi = 0.002$ and $\nu_\omega = 0.02$.

ν_F	0.025	0.038	0.05	0.063	0.075
Level	0.84	0.82	0.82	0.82	0.82
Slope	0.15	0.14	0.15	0.14	0.14
Convexity	0.01	0.03	0.03	0.04	0.04

5.5 Conclusions

In today's financial markets derivatives on different underlying assets with complex payoffs are traded in huge volumes. Standard financial practice employs mathematical risk models such as the Black-Scholes price formula which are built upon oversimplified stochastic models for price dynamics, and then corrected in an ad hoc way to reduce inaccuracies. These imperfections are highlighted by the volatility smile phenomenon. Importantly, in all these models the individual trading behavior is assumed to be irrelevant.

In this chapter, we present a microsimulation model of options markets to explain the origin of the smile. In our model, the typical behavior of the most active options traders, i.e., speculators and arbitrageurs, is adopted and the prices of the options are determined by demand and supply. Notwithstanding its simplicity, the model reproduces the empirical smile curve in terms of its shape and dynamics. Our results suggest that the volatility smile is a natural consequence of traders' heterogeneous behavior and expectations about the future.

In fact, the importance of heterogeneous beliefs for derivatives markets has been empirically disclosed by studies in behavioral finance. See, for example, Sherrin (1999). Our results confirm that individual trading preferences indeed play a critical role in the behavior of the implied volatility curve. These insights will improve the understanding and quantification of the inherent risk of derivatives trading for institutions and investors alike.